Complete Characterization of Molecular Dynamics in Ultrashort Laser Fields

B. Feuerstein,* Th. Ergler, A. Rudenko, K. Zrost, C. D. Schröter, R. Moshammer, and J. Ullrich
Max-Planck-Institut für Kernphysik, D-69029 Heidelberg, Germany

T. Niederhausen and U. Thumm†
James R. Macdonald Laboratory, Kansas State University, Manhattan, Kansas 66506-2604, USA
(Received 11 May 2007; published 10 October 2007)

Reaction Microscope-based, complete, and time-resolved Coulomb explosion imaging of vibrating and dissociating D_2^+ molecules with femtosecond time-resolution allowed us to perform an internuclear distance (R-)dependent Fourier analysis of the corresponding wave packets. Calculations demonstrate that the obtained two-dimensional R-dependent frequency spectra enable the complete characterization of the wave packet dynamics and directly visualize the field-modified molecular potential curves in intense, ultrashort laser pulses.

DOI: 10.1103/PhysRevLett.99.153002 PACS numbers: 33.20.Tp, 32.80.Rm, 33.80.Rv, 42.50.Hz

Recent advances in femtosecond laser technology and tremendous progress in strong-field physics established the basis for novel schemes of imaging, manipulation, and control of ultrafast atomic and molecular processes. Latest pump-probe experiments employing few-cycle laser pulses enabled real-time mapping of nuclear wave packets even for the fastest molecules [1–5]. With the newly-developed attosecond pulses, this method may soon be able to resolve electron dynamics and sub-fs time scales [6,7]. Moreover, the availability of high-quality intense pulses at kHz repetition rates along with compact fs pulse-shaping systems [8] allows one to approach the long-sought goal to optically control chemical reactions by strong-fields. As compared to weak-field control schemes, this method does not imply a narrow bandwidth adjusted for a particular transition and additionally opens the exciting possibility to dynamically modify the potential surfaces of the molecular complex involved in the reaction [9].

One of the most successful theoretical approaches to describe the behavior of a molecular system under the influence of an intense external field is based on the so-called Floquet model [10]. This quasistatic method provides a general and intuitive picture of molecular dynamics on field-modified molecular potential curves, explaining important strong-field-induced phenomena such as, e.g., ''bond-softening'' (BS), above-threshold dissociation (ATD), vibrational trapping, or ''bond-hardening'' (BH) (see [11] and references therein). However, being based on the periodicity of the field, this approach is expected to be only applicable for rather long pulse durations and quasimonochromatic fields. Definitely being not adapted to describe the interaction of broadband few-cycle laser pulses interacting with molecules, it is not suitable for numerous applications, which require ultrashort pulses in order to achieve the time-resolution needed, including state-of-the-art imaging or control experiments.

In this Letter, we demonstrate a novel experimental and theoretical scheme for the complete mapping and characterization of molecular potential curves that are dynamically modified by a 6–7 fs, intense laser pulse. In a proof-of-principles effort, using the deuterium molecular ion, we introduce a technique for imaging the shape of the molecular potential and the nodal structure of its bound vibrational wave function and show how both are modified by shaping the laser field. The method relies on Fourier analysis of the time- and internuclear distance (R)-dependent probability density $\rho(R, t)$ of the D_2^+ nuclear wave packet that can be either calculated or experimentally reconstructed in pump-probe experiments.

In our pump-probe scenario, $\rho(R, t)$ is reconstructed using time-resolved Coulomb explosion imaging (CEI) [1–4,12] (Fig. 1). The first (pump) laser pulse launches an ionic molecular wave packet by ionizing a neutral D_2 molecule from its ground state, thereby projecting its nuclear wave function onto the ground-state potential curve of the molecular ion. Being no longer in an eigenstate, the corresponding wave packet will start to oscillate, and its propagation is monitored by the second (probe) pulse, which, arriving after a certain time delay, removes the second electron and induces Coulomb explosion of the molecular ion. The measured energy release then consists of the Coulomb energy and the kinetic energy at the moment of explosion. Since for the bound wave packet the latter component is rather small, R can be directly reconstructed from the fragment energy using the Coulomb law. Compared to conventional methods of wave packet diagnostic, this technique possesses two decisive advantages. First, it enables a simultaneous mapping of the complete nuclear wave packet provided the probe pulse is chosen intense enough to ensure that all the molecules are ionized independent of R [4,12]. Second, being a measurement in the time domain, it provides additional information about the initial phase of the wave packet [5].

Figure 1(b) shows the D_2^+ wave packet's time-dependent probability density (given by the yield of D^+ pairs measured in coincidence as a function of the pump-probe delay τ) experimentally reconstructed for values of R between

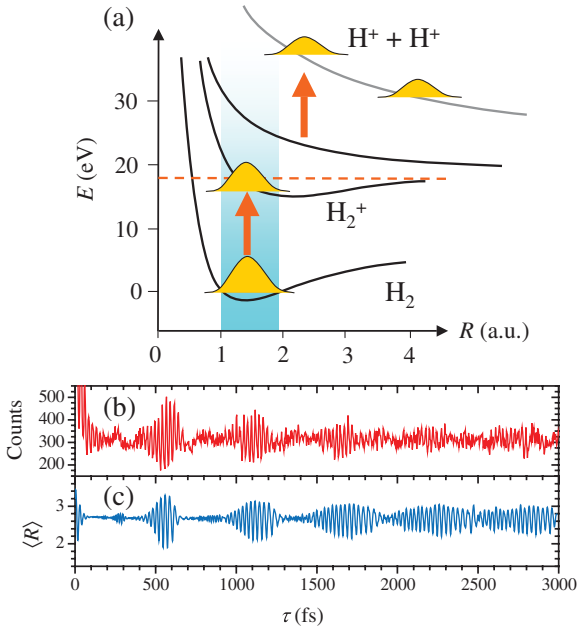

FIG. 1 (color). (a) Pump-probe scheme with CEI of vibrational D_2^+ wave packets. (b) Time-dependent yield of coincident D^+ pairs as function of the pump-probe delay τ for an R interval from 3.5 to 4 a.u. (c) Theoretical expectation value for R the field-free D_2^+ wave packet propagation of an initial Franck-Condon distribution.

3.5 to 4 atomic units (a.u.). Because of the anharmonicity of the D_2^+ potential curve, the corresponding eigenstates are not equally spaced and, thus, instead of a regular oscillation, the wave packet's propagation undergoes cycles of dephasing and revivals [13]. The comparison with Fig. 1(c) shows that our experiment reproduces an earlier model prediction [13] obtained by numerical Crank-Nicholson propagation [14] of the field-free Schrödinger equation starting with an initial Franck-Condon (FC) distribution.

The availability of both measured and calculated time series $\rho(R, t)$ for a wide range of R provides an unprecedented amount of nearly complete information about the nuclear dynamics and, thus, of the field-modified potentials that govern it. The following detailed analysis of this information in terms of elementary process (BS, vibrational excitation, ATD, BH) is of general interest since the evolution of any chemical reaction is defined by wave packet dynamics along a certain reaction coordinate, often over a potential barrier. Provided the time series for a given R is long enough, the wave packet structure in the energy (frequency) domain can be reconstructed via its Fourier transformation. As we will demonstrate below, superimposing the Fourier spectra for all R, one can reveal the complex population amplitudes of the individual vibrational states, the spatial distribution of these states, and their frequency spectrum. Since the latter two are determined by the details of the particular molecular potential, the underlying potential itself can be reconstructed from the experimental observables.

Generally, the wave packet can be represented as a coherent superposition of vibrational states $\chi_v(R)$

$$\Psi(R, t) = \sum_v a_v e^{-i\omega_v t}\chi_v(R) \tag{1}$$

which is fully characterized by the set of (complex) coefficients $\{a_v\}$. The observable time-dependent probability density $\rho = |\Psi|^2$ is

$$\rho(R, t) = \sum_v |a_v|^2|\chi_v|^2 + \sum_{u\neq v} a_u^* a_v \chi_u^* \chi_v e^{i\Delta\omega_{u,v}t}, \tag{2}$$

where $\Delta\omega_{u,v} = \omega_u - \omega_v$. The first time-independent term contains the incoherent diagonal part of the density matrix (in $\{\chi_v\}$ representation) and constitutes the DC-component in our Fourier analysis. The interesting second time-dependent term is a double sum of off-diagonal elements of the density matrix. Subtracting the incoherent part $\rho_{\text{inc}} = \sum_v |a_v|^2|\chi_v(R)|^2$, we introduce the R-dependent harmonic analysis

$$\begin{aligned}\tilde{\rho}(R, \omega; T) &\equiv \frac{1}{\sqrt{2\pi}}\int_0^T dt[\rho(R, t) - \rho_{\text{inc}}]e^{-i\omega t} \\ &= \sqrt{2\pi}\sum_{u\neq v} a_u^* a_v \chi_u^*(R)\chi_v(R)\delta_T(\Delta\omega_{u,v} - \omega),\end{aligned} \tag{3}$$

where $\delta_T(\Omega) \equiv \frac{1}{2\pi}\int_0^T dt e^{i\Omega t}$. This transformation yields the spectrum of vibrational spacings $\sum_{u\neq v}\delta_T(\Delta\omega_{u,v} - \omega)$, the spatial distribution of eigenfunctions $\chi_u^*(R)\chi_v(R)$, and the complex expansion coefficients (population amplitudes and relative phases) $a_u^* a_v$.

Figure 2(a) shows the result of such an analysis in Fourier space as the power spectrum $|\rho(\tilde{R}, f)|^2$ (with $f = \omega/2\pi$) for the simulated field-free propagation of a D_2^+ vibrational wave packet with an initial Franck-Condon distribution. A detailed description of the numerical simulation can be found in [13,15]. In order to compare the results with the available experimental data, the sampling time T was chosen to be 3 ps, enabling sub-meV resolution [4]. In the graph with f on the horizontal and R on the vertical axis, the vibrational frequencies $\Delta f_{u,v} = \Delta\omega_{u,v}/(2\pi)$ appear as a series of vertical lines. Because of the large wave function overlap between successive stationary vibrational states, lines of the $\Delta v = u - v = 1$ series are mapped most distinctly. Because of the anharmonicity of the $1s\sigma_g$ potential curve of D_2^+, they are ordered as $\Delta f_{1,2} > \Delta f_{2,3} > \Delta f_{3,4} > \ldots$.

Since individual vibrational eigenstates only exist within a well-defined range of internuclear distances, beyond which they decay exponentially, the border line of this classically allowed regime marks the lowest adiabatic potential curve ($1s\sigma_g$) of the molecular ion which can be clearly retraced in Fig. 2(a). Closer inspection of (3) reveals also an R-dependent structure in each vertical line in Fig. 2(a) that maps the nodes of the stationary vibrational wave functions. The strength of each line at $\Delta f_{u,v}$ is

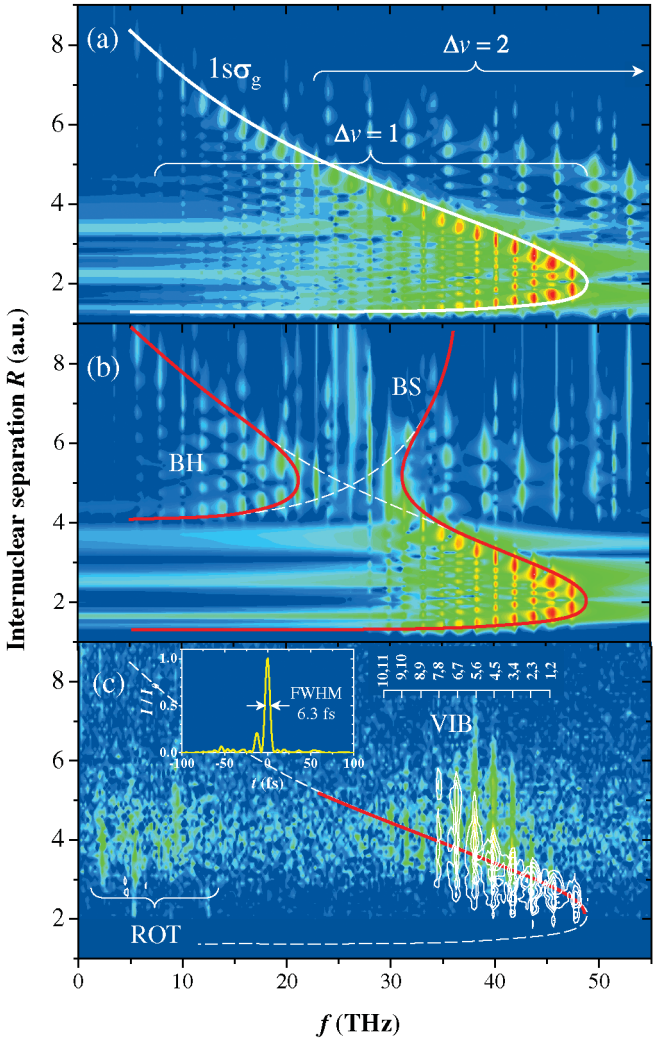

FIG. 2 (color). Two-dimensional power spectrum as function of the frequency f and the internuclear distance R for 3 ps sampling time. (a) numerical field-free wave packet propagation of an initial Franck-Condon distribution. (b) as (a) but with a 50 fs pedestal of 0.01 PW/cm^2 preceding the probe pulse causing "bond softening" (BS) and "bond hardening" (BH). (c) Experimental distribution extracted from coincident D^+ pairs with vibrational (VIB) and rotational (ROT) contributions. White contours: numerical result using the actual laser pulse profile (see inset). All data are shown on a logarithmic scale with a dynamic range of 10^6 (a, b) and 10^3 (c), respectively.

proportional to the product $\chi_u^*(R)\chi_v(R)$ and thus displays all the nodes of both vibrational states involved. If one used the full information in the harmonic analysis (including phases), one could recursively reconstruct all stationary states and complex expansion coefficients, by starting with a Gaussian function for the lowest vibrational state and by normalizing the overall distribution to unity.

Whereas the field-free example discussed above is instructive for the general understanding of our imaging technique, the situation becomes much more interesting in the presence of an external field, where a direct experimental visualization of the field-modified molecular potential becomes feasible. Figure 2(b) shows the harmonic analysis for a model calculation in which a weak laser field of 0.01 PW/cm^2 and 50 fs duration precedes the probe pulse (for any delay). The figure displays a number of differences compared to the field-free case: a second light-induced potential well in the region of the upper vibrational states and the opening of a gap around 25 THz through which the molecular ion can dissociate, as seen from the significant probability density in a region, which is classically forbidden in the field-free case. Some signatures of these features have been observed in a number of earlier experiments and are often discussed in terms of the Floquet picture mentioned above [10]. Because of the interaction with the laser field, the two lowest-lying field-free potential curves combine and form new light-induced potential curves which can temporarily trap part of the density (BH) or allow dissociation via an opened avoided crossing (BS). We note that the situation discussed above is inherently realized in any kind of a realistic pump-probe experiment, since sub-1 fs few-cycle laser pulses employed as a probe almost unavoidably sit on a rather long (50–100 fs) pedestal of at least 1% of the pulse peak intensity [2,3,16].

Figure 2(c) shows the result of the Fourier analysis of our experimental data. Details of the setup as well as of the R-reconstruction procedure can be found in [3,4]. We used pump and probe pulses of 0.3 and 0.6 PW/cm^2, respectively, both 6–7 fs long. The delay, scanned from 0 to 3 ps, was determined with an absolute precision of less than 0.3 fs. By measuring the autocorrelation directly at the reaction volume, using the ion rate as nonlinear signal, we verify *in situ* the length of the pulse and monitor the absolute time zero of the delay over 80 hours of data acquisition. The actual pulse profile (inset) with a significant prepulse was determined using the SPIDER technique [17].

Clear vertical lines are visible in the experimental data, corresponding to pairs of vibrational states from $\Delta f_{1,2}$ [denoted by 1,2 in Fig. 2(c)] to $\Delta f_{10,11}$ with measured frequencies being in excellent agreement with the known spectroscopic data for the field-free D_2^+ [18]. Because of ionization suppression at smaller R [3–5,15], we can only observe probability densities of bound vibrational states close to the *outer* classical turning point in the field-free potential (solid red line). In addition, we find large probability densities outside the field-free boundary indicating laser-induced dissociation. This dissociation occurs most likely near $v = 4 \ldots 6$, in agreement with previous experimental evidence [4]. Besides the vibrational lines, we even identify weak lines below 10 THz as rotational excitations [4] that are not included in the present calculations.

In order to simulate the experimental results, we have included the actual pulse shape into the theoretical modeling both for the pump and the probe pulse. The initial wave packet is prepared according to analytical R-dependent ADK ionization rates, and the following propagation includes the trailing half of the pump pulse. For the probe pulse, the R-dependent ionization rate [15] is taken into

account for the population of the CE channel which resembles the effect of ''charge-resonant enhanced ionization'' [19], significantly enhancing ionization at internuclear distances between 4 and 6 a.u. The result, shown as white contour lines in Fig. 2(c), agrees remarkably well with the experimental data.

While the results of Fig. 2(b) were found to be essentially consistent with the predictions of the Floquet [10] model, the experimental as well as theoretical data presented in Fig. 2(c) manifest considerable deviations, both for BH and BS regions. For BS, the range of vibrational states contributing to dissociation in the Floquet description would correspond to the opening of an avoided crossing via absorption of three photons. However, the measured kinetic energies of the dissociating fragments [4,20] are considerably lower than those expected (and observed for longer pulse durations) for the three-photon Floquet channel [11]. Thus, as might have been expected, we are led to conclude that the time-averaged Floquet model cannot describe ultrafast molecular dynamics induced by a few-cycle, shaped perturbing field with its broad photon frequency spectrum and distinct time dependence.

At this point, one might wonder why the observed vibrational frequencies agree so well with the spectroscopic data for field-free D_2^+ [18]. The reason is that the measured frequencies are defined by propagation during the whole sampling time interval of pump-probe delays, during most of which the nuclear wave packet experiences the field-free potential well. Thus, the R-dependent power spectra in Figs. 2(b) and 2(c) image, for the first time, a *distorted* molecular potential curve during the short femtosecond time interval of the perturbing probe laser (pre-)pulse.

In conclusion, we have demonstrated in a combined experimental and theoretical proof-of-principle effort a novel method for ultrafast imaging of molecular potentials modified by a strong time-dependent external field. This has been achieved using the internuclear-distance-resolved Fourier transformation of the time-dependent D_2^+ wave packet density probability, reconstructed via CEI. In contrast to other schemes of two-dimensional Fourier analyses (see, e.g., [21]), our probing technique (time-resolved CEI) is sensitive to the wave packet motion over a wide range of R, making this approach capable of providing spatial and spectral information simultaneously. Using a D_2^+ vibrational wave packet as a demonstrative example, we illustrate that our imaging procedure retraces the shape of the lowest field-distorted potential curves of the molecular ion. Evidence is provided that, under certain conditions, the method can even reveal the nodal structure of bound vibrational states. The technique is applicable for any strong dynamical perturbation without restrictions with respect to the perturbing field profile, and on time scales only limited by the duration of the effective probe pulse. Similar harmonic analysis of CEI experiments with upcoming attosecond pulses [7] resembling delta-pulses on a molecular time scale, will essentially remove the influence of the probe pulse, and, therefore, allow the investigation of both the field-free propagation of the molecular wave-packet and the potential structure under the influence of any external field applied prior to the probe pulse.

Extending the technique to more complicated polyatomic molecular systems or reacting complexes, enabled by modern 3D experimental imaging techniques [2,22,23], will allow one to investigate molecular dynamics across the (field-modified or field-induced) potential barrier along a particular reaction coordinate and, thus, provide a basis for novel schemes of multidimensional optical control of reactions.

T. N. and U. T. acknowledge the support by the NSF (Grant No. PHY-0354840) and the Division of Chemical Sciences, Office of Basic Energy Sciences, Office of Energy Research, US DOE.

*feuerstb@mpi-hd.mpg.de
†thumm@phys.ksu.edu

[1] A. S. Alnaser *et al.*, Phys. Rev. A **72**, 030702(R) (2005).
[2] F. Légaré *et al.*, Phys. Rev. A **72**, 052717 (2005).
[3] A. Rudenko *et al.*, Chem. Phys. **329**, 193 (2006).
[4] Th. Ergler *et al.*, Phys. Rev. Lett. **97**, 193001 (2006).
[5] Th. Ergler *et al.*, Phys. Rev. Lett. **97**, 103004 (2006).
[6] P. Agostini and L. F. DiMauro, Rep. Prog. Phys. **67**, 813 (2004).
[7] C. D. Lin, X. M. Tong, and T. Morishita, J. Phys. B **39**, S419 (2006).
[8] A. Präkelt *et al.*, Rev. Sci. Instrum. **74**, 4950 (2003).
[9] R. J. Lewis, G. M. Menkir, and H. Rabitz, Science **292**, 709 (2001).
[10] S. R. Barone, M. A. Narcowich, and F. J. Narcowich, Phys. Rev. A **15**, 1109 (1977).
[11] J. H. Posthumus, Rep. Prog. Phys. **67**, 623 (2004).
[12] S. Chelkowski, P. B. Corkum, and A. D. Bandrauk, Phys. Rev. Lett. **82**, 3416 (1999).
[13] B. Feuerstein and U. Thumm, Phys. Rev. A **67**, 063408 (2003).
[14] W. H. Press, S. A. Tenkolsky, W. T. Vetterling, and B. F. Flannery, *Numerical Recipies* (Cambridge University Press, Cambridge, 1992).
[15] T. Niederhausen and U. Thumm, Phys. Rev. A (to be published).
[16] B. Schenkel *et al.*, Opt. Lett. **28**, 1987 (2003).
[17] C. Iaconis and I. A. Walmsley, Opt. Lett. **23**, 792 (1998).
[18] G. Hunter, A. W. Yau, and H. O. Pritchard, At. Data Nucl. Data Tables **14**, 11 (1974).
[19] T. Zuo and A. D. Bandrauk, Phys. Rev. A **52**, R2511 (1995).
[20] A. Rudenko *et al.*, J. Phys. B **38**, 487 (2005).
[21] M. J. J. Vrakking, D. M. Villeneuve, and A. Stolow, Phys. Rev. A **54**, R37 (1996).
[22] A. Hishikawa, A. Iwamae, and K. Yamanouchi, Phys. Rev. Lett. **83**, 1127 (1999).
[23] T. Osipov *et al.*, J. Mod. Opt. **52**, 439 (2005).